J Membrane Biol (2012) 245:651–659
DOI 10.1007/s00232-012-9487-6

Molecular-Level Characterization of Lipid Membrane Electroporation using Linearly Rising Current

Peter Kramar · Lucie Delemotte · Alenka Maček Lebar · Malgorzata Kotulska · Mounir Tarek · Damijan Miklavčič

Received: 19 December 2011 / Accepted: 5 July 2012 / Published online: 11 August 2012

Abstract We present experimental and theoretical results of electroporation of small patches of planar lipid bilayers by means of linearly rising current. The experiments were conducted on ~120-μm-diameter patches of planar phospholipid bilayers. The steadily increasing voltage across the bilayer imposed by linearly increasing current led to electroporation of the membrane for voltages above a few hundred millivolts. This method shows new molecular mechanisms of electroporation. We recorded small voltage drops preceding the breakdown of the bilayer due to irreversible electroporation. These voltage drops were often followed by a voltage re-rise within a fraction of a second. Modeling the observed phenomenon by equivalent electric circuits showed that these events relate to opening and closing of conducting pores through the bilayer. Molecular dynamics simulations performed under similar conditions indicate that each event is likely to correspond to the opening and closing of a single pore of about 5 nm in diameter, the conductance of which ranges in the 100-nS scale. This combined experimental and theoretical investigation provides a better quantitative characterization of the size, conductance and lifetime of pores created during lipid bilayer electroporation. Such a molecular insight should enable better control and tuning of electroporation parameters for a wide range of biomedical and biotechnological applications.

Keywords Planar lipid bilayer · Linear rising current · Molecular dynamics simulation

P. Kramar · A. Maček Lebar · D. Miklavčič (✉)
Faculty of Electrical Engineering, University of Ljubljana, Trzaska 25, 1000 Ljubljana, Slovenia
e-mail: damijan.miklavcic@fe.uni-lj.si

L. Delemotte · M. Tarek (✉)
UMR Structure et Réactivité des Systèmes Moléculaires Complexes, Centre National de la Recherche Scientifique, Université de Lorraine, Nancy, France
e-mail: mounir.tarek@univ-lorraine.fr

M. Kotulska
Institute of Biomedical Engineering and Instrumentation, Wroclaw University of Technology, Wybrzeze Wyspianskiego 27, 50-350 Wroclaw, Poland

Introduction

Electroporation is a process in which lipid membranes, the cell envelopes, are permeabilized when subjected to high electric fields (Neumann and Rosenheck 1972). Under specific conditions, Electroporation may be reversible, in which case membranes and cells recover their initial state when the applied field is turned off (Zimmermann et al. 1976; Glaser et al. 1988). Electroporation is widely used in biomedicine and biotechnology to enhance the transport of molecules across the plasma membrane (Prausnitz et al. 1993), a technique also known as electropermeabilization (Mir et al. 1988; Teissie et al. 1999). Applications range from in vitro DNA plasmids and siRNA cell delivery (Golzio et al. 2002; Villemejane and Mir 2009) to clinical electrochemotherapy (Marty et al. 2006), where delivery of drugs, e.g., bleomycin and cisplatinum, to cancer cells is enhanced (Mir et al. 1995; Sersa et al. 1995; Heller et al. 1999). It is now well established that the efficiency of such applications depends on the intensity, duration and number of electric pulses applied (Rols and Teissie 1998; Pucihar et al. 2002; Teissie et al. 2008). Better control and tuning of the method require full understanding and quantitative characterization of the molecular-level processes taking place during and after electroporation.

Low-intensity electric fields normal to the membrane induce, through Maxwell-Wagner polarization (Kotnik et al. 1997), a transmembrane voltage. When the voltage reaches a certain value characteristic of the membrane composition, water wires form within the bilayer. This is followed by the appearance of hydrophilic pores that disrupt the membrane integrity, as suggested by early molecular dynamics (MD) simulations (Tieleman et al. 2003; Tarek 2005). Electroporation voltage thresholds are most often determined in experiments where electric pulses or linearly increasing voltage signal is applied to planar lipid bilayers (Kramar et al. 2007) or on cells in vitro using fluorescent dyes (Teissie and Rols 1993) or cytotoxic drugs (Kotnik et al. 2000). However, most often, such techniques do not allow characterization of structural and dynamic properties of the putative pores formed during the membrane electroporation, such as pore size, conductance and lifetime. As an alternative, electroporation under constant current conditions has been proposed (Genco et al. 1993; Kalinowski et al. 1998). This method allows the maintenance of long-lived fluctuating pores, as shown for planar membranes of lecithin (Koronkiewicz and Kalinowski 2004; Kotulska et al. 2004, 2007).

Here, we report on electroporation of planar lipid bilayer patches by another experimental protocol, based on exposure to linearly rising current (Koronkiewicz et al. 2002). We studied the appearance of pores and investigated the molecular mechanism of electroporation. Exposing lipid bilayers to a linearly increasing current builds voltage across the membrane and induces events indicative of poration and subsequent resealing of the bilayer. In order to characterize these changes on a molecular scale, we carried out MD simulations under similar conditions. Combined together, the theoretical and experimental investigations allowed a quantitative estimation of the properties of the created pores.

Materials and Methods

Experiments on Planar Lipid Bilayer

Experiments under current-controlled conditions (i.e., current clamp) were performed using a measuring system (Fig. 1), as described by Kalinowski and Figaszewski (1995a, b) and Kalinowski et al. (1998), with four Ag–AgCl electrodes (two current electrodes and two reference electrodes). The measuring system consisted of two modules. The first one was a capacity to period converter, used for measuring the bilayer's capacitance; the second was a potentiostat-galvanostat for current-controlled planar lipid bilayer studies.

The chamber where planar lipid bilayers are formed consists of two 5.3-cm^3 reservoirs made of Teflon. Between the two compartments, a thin Teflon sheet with a

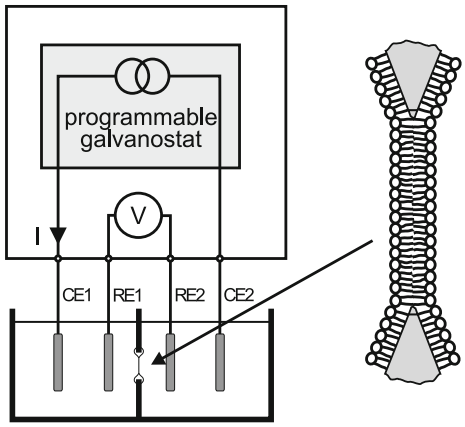

Fig. 1 Measurement system with a programmable galvanostat and a voltameter with four Ag–AgCl electrodes, two current electrodes (*CE*) and two reference electrodes (*RE*) plunged into the Teflon chamber compartments

117-μm diameter, round aperture was inserted (Kramar et al. 2009). Planar lipid bilayers were formed by the Montal–Mueller method (Montal and Mueller 1972).

We studied bilayers prepared from 1-pamitoyl 2-oleoyl phosphatidylcholine (POPC) (Avanti Polar-Lipids, Alabaster, AL). Lipid powder was dissolved in a 9:1 hexane/ethanol solution. A 3:7 mixture of hexadecane and pentane was used for torus formation. The salt solution consisted of 0.1 M KCl and 0.01 M HEPES in the same proportion. We added 1 M NaOH to obtain a neutral pH (7.4).

Measuring protocols consisted of two parts: capacitance measurement and lipid bilayer breakdown voltage measurement. Membrane capacitance was measured with the capacitance to period converting principle described in detail by Kalinowski and Figaszewski (1995a) and then normalized to the surface area of the bilayer to calculate the specific capacitance (C_{BLM}). We then determined the breakdown voltage (U_{br}) of each lipid bilayer by applying linear rising current signals (of slope k). Nine different slopes were selected: 0.03, 0.05, 0.1, 0.2, 0.5, 4, 8, 10 and 20 μA/s. U_{br} was defined as the voltage at t_{br}, when an abrupt voltage drop due to lipid bilayer rupture was detected (Fig. 2).

Electrical Model of Experimental Setup

The whole measuring system was modeled by an equivalent electrical circuit (Fig. 3). We used Spiceopus software (http://www.spiceopus.com/) to simulate the equivalent electrical circuit behavior under our specific experimental conditions (Tuma and Buermen 2009). In the Spiceopus model (Fig. 3) current was applied by current generator I_0. In Fig. 3, C_{BLM} is the capacitance of the planar lipid bilayer, R_{BLM} is the resistance of the planar lipid bilayer,

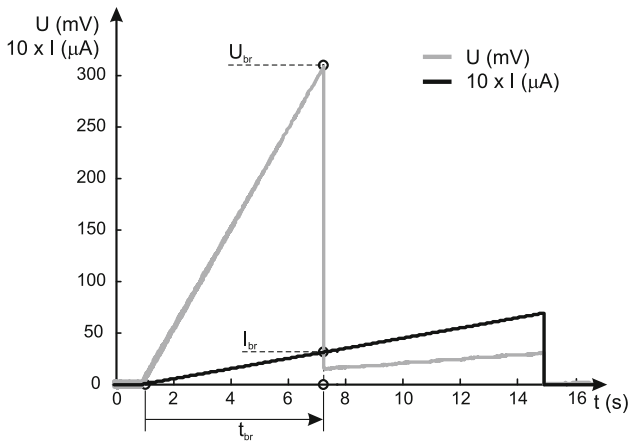

Fig. 2 Breakdown voltage U_{br} determination by means of linear rising current signal

C_{sys} is the capacitance of the chamber, R_{sys} is the resistance of the chamber and R_P is resistance of the pores.

Spiceopus software uses node-voltage analysis. To measure the currents flowing through various parallel branches of the circuit, an independent voltage source ($V = 0$) was added in series with the element of the branch (Fig. 3) according to recommendations. The appearance of pores (R_P) in the planar lipid bilayer was simulated by introducing a voltage-controlled switch in the R_P branch. An intact planar lipid bilayer was represented by an open switch, while a porated planar lipid bilayer was represented by a closed switch.

The value of R_{BLM} was set to 10^8 Ω, which is the typical value found in the literature (Tien 1974). The value of membrane capacitance was estimated to be 0.51 μF/cm^2 as an average of the experimentally measured values. Values for C_{sys} and R_{sys} were obtained by optimization in Spiceopus software. The values that gave the best fit are $C_{sys} = 105 \pm 54$ nF and $R_{sys} = 100 \pm 5$ kΩ. Finally, R_P, i.e., the conductance of pores ($1/R_P$) value in the model, was adjusted to each of 44 experimentally obtained voltage drops.

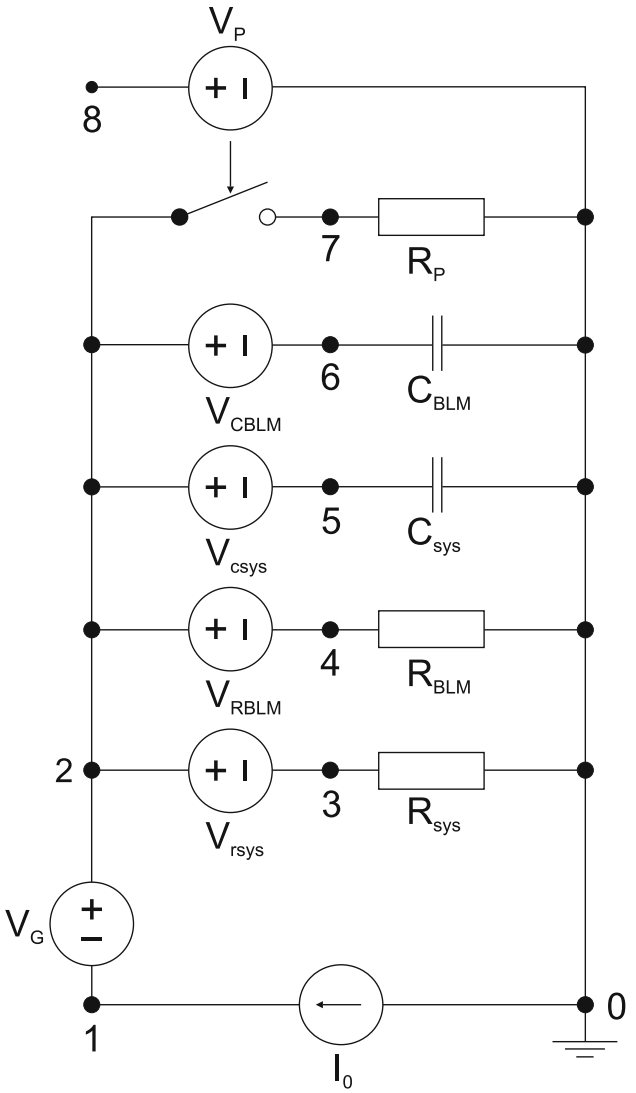

Fig. 3 Equivalent electrical circuit representing the measurement chamber (R_{sys}, C_{sys}) and the planar lipid bilayer (R_{BLM}, C_{BLM}) used for the SPICE model. The current source I_0 was used to simulate current-clamp conditions. A voltage control switch (V_P) was used to simulate a pore on the planar lipid bilayer. Voltage generators V_G, V_{rsys}, V_{RBLM}, V_{csys} and V_{CBLM} with voltage set to zero were introduced to measure the current trough in each branch

MD Simulations

The membrane model used for this study is an equilibrated fully hydrated POPC bilayer and was built by replication of a previous well-equilibrated smaller system (Delemotte et al. 2008). It consists of 1,152 lipid units and 58,304 water molecules organized in two lamellae above and below the lipids. At the temperature set for the study, i.e., 300 K, the bilayer was in the biologically relevant liquid crystal Lα phase. The solvent contained 560 Na^+ and 560 Cl^- ions. The final dimensions of the system before extending it in the z direction were 168 × 183 × 110 Å^3 and the total number of atoms was 261,280.

The MD simulation was carried out using the program NAMD targeted for massively parallel architectures (Kale et al. 1999; Phillips et al. 2005). The systems were examined at constant pressure and constant temperature (1 atm and 300 K) or at constant volume and constant temperature (300 K) employing Langevin dynamics and the Langevin piston method. The equations of motion were integrated using the multiple time-step algorithm. A time step of 2.0 fs was employed. Short- and long-range forces were calculated every two and four time steps, respectively. Chemical bonds between hydrogen and heavy atoms were constrained to their equilibrium value. Long-range,

electrostatic forces were taken into account using a fast implementation of the particle mesh Ewald (PME) method (Darden et al. 1993; Essmann et al. 1995), with a direct space sum tolerance of 10^{-6} and a spherical truncation of 11 Å. Water molecules were described using the TIP3P model (Jorgensen et al. 1983), and a united-atom representation was adopted for the acyl chains of the POPC lipid molecules (Henin et al. 2008).

The system was first equilibrated for tens of nanoseconds at constant temperature (300 K) and constant pressure (1 atm), as in the simulations of multilamellar stacks of lipids. Following this equilibration, the initial salt concentration (~530 mM, counting only the fraction of ions) went down in the bulk, because of accumulation of charges near the zwitterionic lipid headgroup interface, to 490 mM. The system size was then extended in the z direction ($L_z = 200$ Å), creating therefore an air–water interface. Subsequent simulations were run at constant volume, using 3D periodic boundary conditions, the thickness of the vacuum slab created above and below the solvent (>40 Å each) being large enough to prevent significant interactions between the original cell and its replicas in the z direction, i.e., perpendicular to the bilayer (Fig. 4).

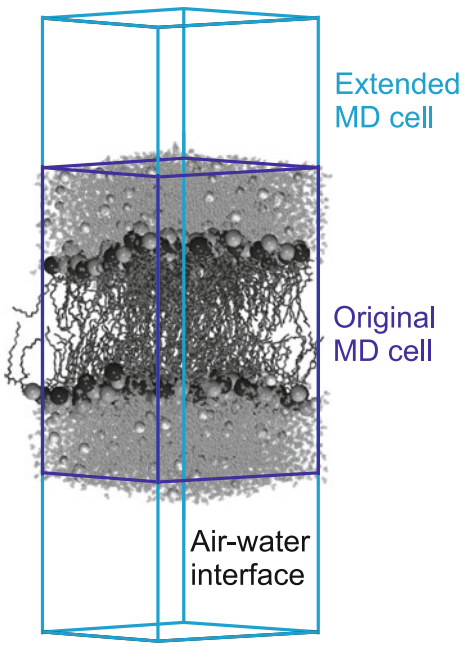

Fig. 4 MD simulation setup: configuration of a hydrated POPC lipid bilayer embedded in a ~500-mM NaCl electrolyte solution. Lipid tails are depicted as *purple sticks*, and headgroup atoms are represented as *large spheres* (*cyan* choline, *blue* phosphate). Water molecules are represented as *gray* and Cl^- and Na^+ ions as, respectively, *cyan* and *yellow small spheres*. The extension of the simulation cell (from *purple* to *blue box*) creates air–water interfaces that permit induction of a transmembrane voltage by imposing a net charge imbalance across the bilayer (Color figure online)

Further simulations were performed using the standard "electric field method" for which a constant electric field, $\vec{E}$, normal to the bilayer, was applied on the "nonextended" systems (i.e., original MD cell) using 3D periodic boundary conditions. Under $E \sim 0.2$ V Å^{-1}, the applied voltage is $U = E{\cdot}L_z$, where L_z is the length of the simulation box along the normal to the bilayer and amounts here to ~2 V. For an MD simulation under such conditions lasting about 2 ns, the diameter of the hydrophilic pore increased to ~50 Å.

The one-dimensional electrostatic potential profile along the membrane normal was derived directly from the MD simulations as a double integral of the charge distribution of all atoms averaged over the membrane planes, $\rho(z)$, as

$$\Phi(z) - \Phi(0) = -\varepsilon_0^{-1} \int \int \rho(z'')dz''dz'$$

As a reference, $\Phi(z)$ was set to zero in the upper electrolyte. Considering the present protocol, $\Phi(z)$ showed plateau values in the aqueous regions. The difference between the plateau values at the two electrolytes corresponds to the transmembrane potential, ΔV.

Results

We performed 63 experiments at nine different slopes of linearly rising current (0.03, 0.05, 0.1, 0.2, 0.5, 4, 8, 10 and 20 μA/s) during which the transmembrane voltage, U, across the planar lipid bilayer was monitored. For each bilayer, the capacitance was first estimated from measurements of the whole system capacitance with and without bilayer formed (Kramar et al. 2009; Benz and Janko 1976), using the capacitance to period converter method (Kalinowski and Figaszewski 1995b).

A typical trace of the voltage measured across the bilayer, corresponding to the applied current, is presented in Fig. 5a. As expected, at a certain U_{br}, high enough transmembrane voltage, the voltage collapses, indicating a breakdown of the planar lipid bilayer. In about half of the experiments, at some voltage level U_d below U_{br}, the transmembrane voltage suddenly drops for a few millivolts (within the experimental time resolution of either 1 or 10 ms). Afterwards, the voltage either continues rising with the same slope as previously before reaching U_{br} and collapsing to ~0 mV or, after increasing steadily for a while, jumps back to a higher value and then exhibits the same rise as before U_d (Fig. 5a). Interestingly, as opposed to the constant current-clamp method for which we previously observed only fluctuations in the transmembrane voltage (Kotulska et al. 2004, 2007, 2010), this new linearly rising current excitation enables observation of well-defined and reproducible events.

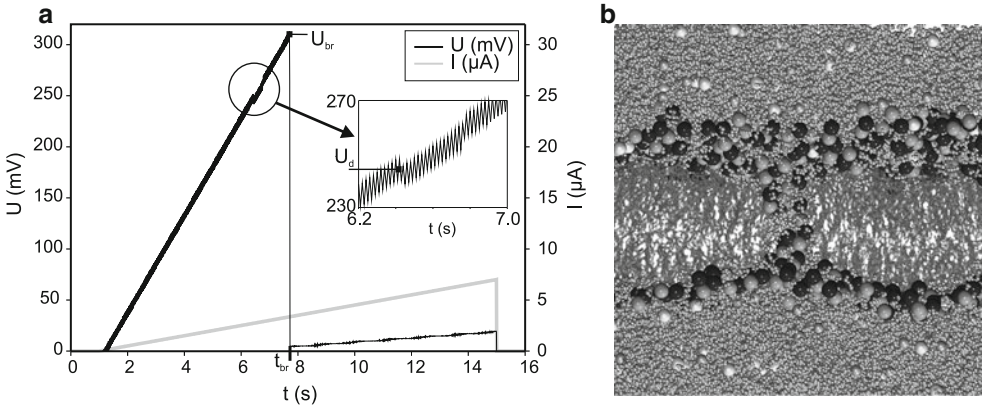

Fig. 5 **a** Trace of the measured transmembrane voltage (U) under linearly rising current (I) conditions. U_{br} is the voltage at which bilayer breakdown occurs, and the *arrow* points at a transient voltage drop. After this event, the bilayer appears to recover completely within a fraction of the second. **b** MD simulation snapshot of the hydrophilic pore created in the POPC bilayer subject to high transmembrane voltages induced by ionic imbalance. Same color code as Fig. 4

Out of these 63 experiments, small voltage drops (as examples indicated by arrows in Fig. 6) were observed in 31 experiments. Mostly we observed a single voltage drop, but even up to three separate drops were observed in these experiments. All together, we recorded 44 small voltage drops. According to their shape, they were divided into two categories: (1) drop only and (2) drop and reseal (Table 1). At drop only (Fig. 6a) the voltage drops to a finite value of U_d and does not rise back. At drop and reseal (Fig. 6b) the voltage drops for a finite value of U_d; after a certain time interval t event, the voltage rises back to a value of U_{rise}, continuing on the same slope as before the drop.

In order to quantify these voltage drop events and to discriminate between the contribution of the measurement chamber and that of the bilayer, it was necessary to model the whole system using an equivalent electrical circuit. A SPICE model including five parallel branches connected to a current generator (Fig. 3) was used to model the changes in the recorded voltage of all 63 performed experiments. Two branches of the circuit describe the measurement system, as a capacitor C_{sys} in parallel with a resistor R_{sys}. The values for C_{sys} and R_{sys} were iteratively optimized to fit the experimental curves obtained in the experiments, where poration events occurred at U_d and equalled 105 ± 54 nF and 100 ± 5 kΩ, respectively. The three other branches were introduced to describe the membrane as (1) a capacitor (C_{BLM}), (2) a resistor (R_{BLM}) and (3) a resistor (R_P) and a switch in series. This last branch models the bilayer in either an intact or porated state, which corresponds to the switch being opened or closed, respectively. An average value of ∼0.51 μF/cm^2 obtained from all measurements on the lipid membrane was considered for the membrane capacitance (C_{BLM}), and the membrane resistance (R_{BLM}) was ∼10^8 Ω, a value commonly used in the literature to describe membranes (Tien 1974). Finally, the R_P values were adjusted to model the voltage drops occurring at U_d (Table 2; Fig. 7). Using the traces of the recorded voltages, the spice model allowed us to estimate the conductance ($G_P = 1/R_P$) of the pores created at U_d, the distribution of which is reported in Fig. 8.

Quite interestingly, the conductances recorded for planar lipid membranes are much larger than those reported using other protocols, such as current clamp or rising voltage, which range from a fraction of a nanoSiemens (Kotulska et al. 2010; Melikov et al. 2001) to a few tens of nanoSiemens (Kalinowski et al. 1998).

In order to gain insight into the corresponding process taking place at the molecular level, we carried out fully atomistic MD simulations under conditions similar to the experiment. We considered a POPC planar lipid bilayer embedded in a 150 mM NaCl solution. Overall, the system consisted of 1,152 lipids, 58,304 water molecules, 560 sodium ions and 560 chloride ions (a total of 261,280 atoms). The bilayer was first replicated in 3D and equilibrated at a constant pressure (1 atm) and temperature (300 K). Then, it was extended in the z direction (16.8 × 18.3 × 20.1 nm^3) in order to create air (vacuum)–water interfaces (Fig. 4). This setup (Delemotte et al. 2008) enables the generation of a transmembrane voltage by imposing a charge imbalance between the solutions on either side of the membrane. MD simulations performed at different transmembrane voltages (charge imbalances, Q_s) showed that, as such, the POPC membrane behaves as a capacitor (Delemotte et al. 2008). Its capacitance, estimated by $V = Q_s/C$ amounts to 0.85 μF/cm^2.

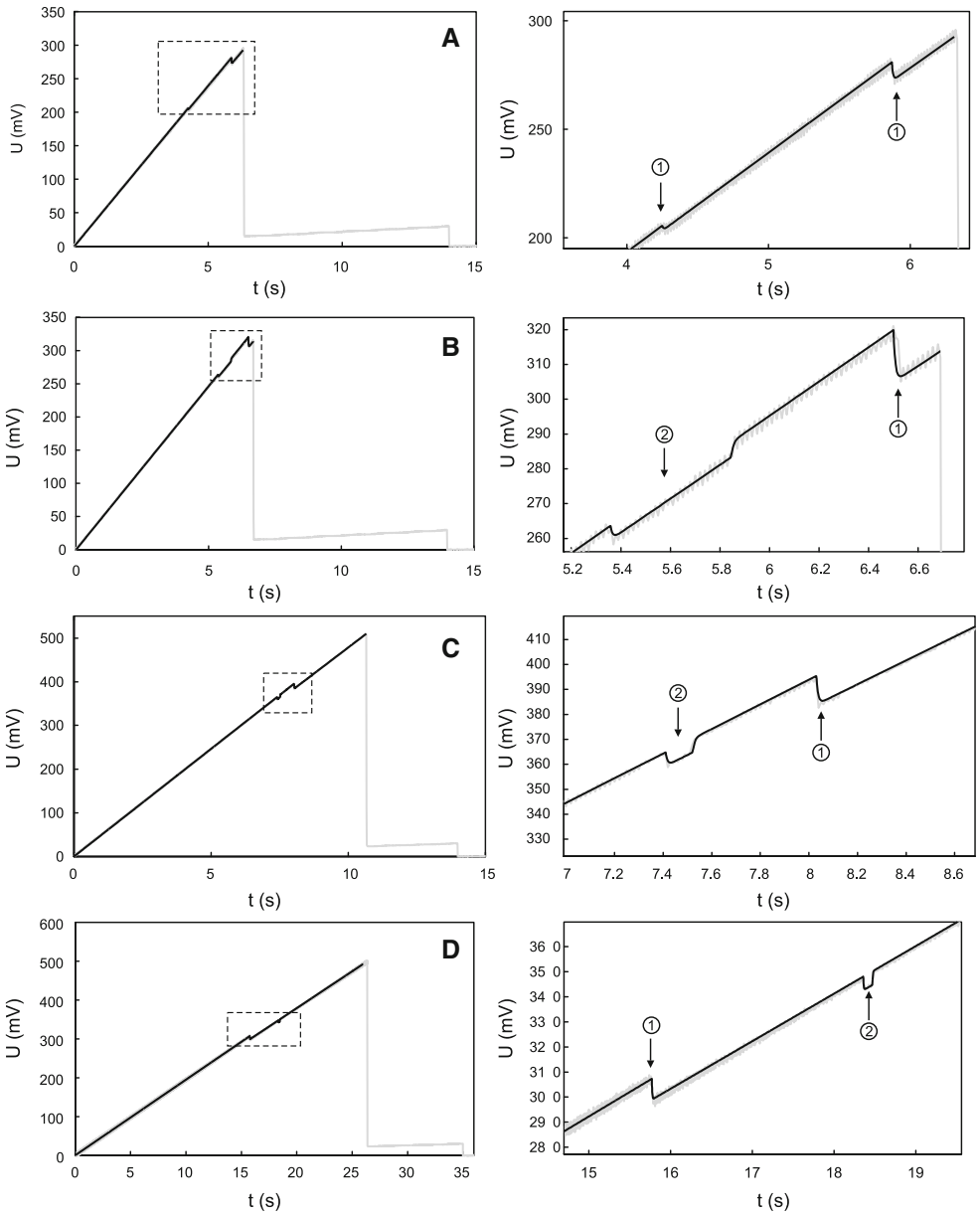

Fig. 6 Experimentally obtained voltage traces (*light lines*) and best fits (*bold lines*) obtained with the SPICE model. The entire voltage traces are presented in the *left column* and a zoom on the event(s) on the *right*

Discussion

As we were mainly interested in characterizing the voltage drop events (Fig. 6, 7), the MD simulations were carried out in order to follow the dynamics of pore creation. Accordingly, we generated systems at transmembrane voltages (ΔV) high enough to induce electroporation, mimicking therefore the experimental event starting at U_d. Using the SPICE model, the intensity of the current applied to the membrane was estimated to be in the order of a few picoamperes (Table 2). Considering the ratio between the sizes of the simulation and experimental membrane patches, this is equivalent to charging the MD patch at a rate of $\sim 10^{-7}$ elementary charges per picosecond. On the simulation time scale (tens of nanoseconds), one should therefore not expect a voltage buildup. Accordingly, the initial charge imbalance imposed to create ΔV was not modified during the simulation run.

Comparison of capacitances estimated in MD simulations (0.85 μF/cm^2) to the experimental values (0.51 μF/cm^2) indicates that the setup and the MD force field we used yielded good agreement with the experiment.

For ΔV above a threshold of 1.5 V, the bilayer undergoes a drastic change in terms of its molecular structure, which is comparable to what was observed when applying an electric field to MD bilayer setups (Tarek 2005;

Table 1 Voltage drops as a function of the linearly rising current slopes

I slopes (k) (μA/s)	Experiments	Total drop events	Drop only	Drop and reseal
0.03	4	4	6	0
0.05	9	6	3	5
0.1	5	1	0	1
0.2	8	3	2	3
0.5	13	10	6	8
4	5	4	5	1
8	5	3	2	2
10	6	0	0	0
20	8	0	0	0

The number of measurements for each current slope, the number of experiments that exhibit voltage drops, including the number of drop-only events and the number of drop-and-reseal events are presented

Table 2 Parameters of the trace (fit) shown in Fig. 7

	t_1	t_2	t_3	t_4	t_5	t_6
t (s)	5.40	5.42	5.57	5.72	5.74	5.84
U (mV)	265.96	264.92	271.65	279.23	282.30	287.91
I (μA)	2.70	2.71	2.78	2.86	2.87	2.92
I_{RSYS} (μA)	2.69	2.68	2.75	2.83	2.86	2.92
I_{RBLM} (pA)	2.66	2.65	2.72	2.79	2.82	2.88
I_{CSYS} (nA)	6.20	2.49	6.14	6.14	13.00	6.20
I_{CBLM} (pA)	2.71	1.09	2.68	2.68	5.68	2.71
I_P (nA)	0.00	26.49	27.17	27.92	0.00	0.00

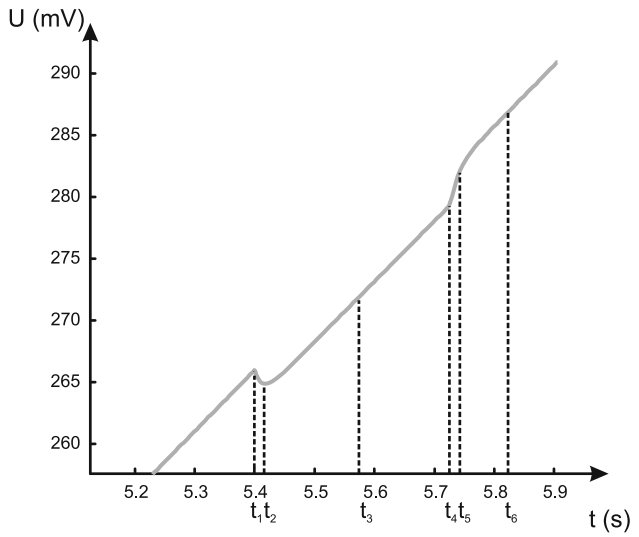

Fig. 7 Example of fit to the recorded traces of voltage (V) as a function of time (s) for event 2 in Fig. 6c

Tieleman 2004; Bockmann et al. 2008; Ziegler and Vernier 2008) or with the charge imbalance method (Gurtovenko and Vattulainen 2005; Kandasamy and Larson 2006; Tarek

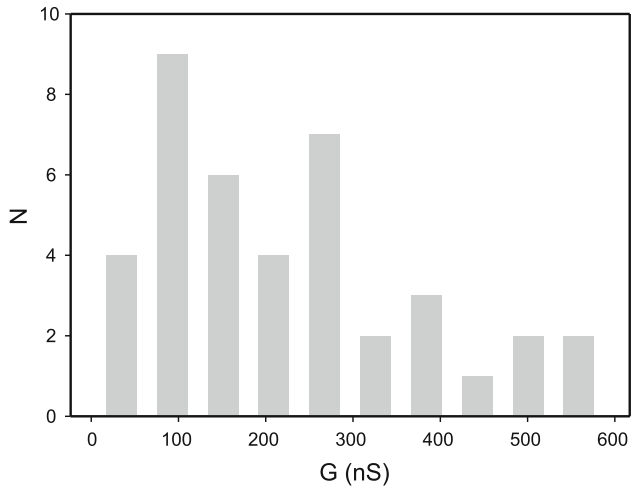

Fig. 8 Distributions of pores conductance $G_P = 1/R_p$ extracted from the SPICE model

and Delemotte 2010). See Gurtovenko et al. (2010) for a review. Indeed, within a few nanoseconds, water fingers started protruding from both sides of the membrane, until a water wire connected the two baths. During the next step, lipid headgroups dived along the sides of these water wires, thus forming a hydrophilic pore. The diameter of the created hydrophilic pore ($\sim$20 Å) was large enough to enable conduction of Na^+ and Cl^- ions from one side of the bilayer to the other, releasing the electrical stress imposed by the ionic imbalance. Accordingly, the initial charge imbalance decreased, leading to a decrease of the transmembrane voltage. When the latter reached values of a few hundred millivolts, the pore stopped conducting ions and the water within the pore retracted toward the external baths, leading to a collapse of the hydrophilic pore. The final topology of the pore toward the end of the simulations remained stable for time spans exceeding 10 ns. It was probably because, as reported in previous simulations, complete recovery of the membrane requires a much longer time scale. We estimated the conductance of the pore, $G_{pMD} = I/U$, where I is the total number of ion translocations over the time elapsed during the simulation. Here, 20 elementary charges were conducted over 10 ns, leading to a value of $I \sim 320$ pA. During these translocations, the voltage dropped from 2 V to 200 mV, leading to values of G_{pMD} ranging from $\sim$160 pS to 1.6 nS in the case of the higher estimate.

Now, what is the most likely explanation, based on the simulation results, for what happens to the bilayer patch at and above the voltage U_d in the experiment? The estimated pore conductance values, obtained in experiments, are in the 100-nS range (Fig. 8). This leads to two hypotheses that may rationalize the observed voltage drops. (1) Multiple pores, such as those observed in MD, are created. The ratio

between experimental and simulation conductance values yields numbers ranging between $\sim$60 and $\sim$600 pores in the experimental patch, which corresponds to pore densities of $\sim 600 \times 10^8$ pore/m^2. Interestingly, a similar pore density was estimated from earlier measurements assuming the formation of hydrophilic pores of 1-nm diameter (Glaser et al. 1988). (2) At each drop event, a single pore is created in the experimental patch, the topology of which is different from the one obtained in the simulation. Its size allows for a conductance 60–600 times larger than that of the MD simulations. The single pore would then enable conduction of 120 elementary charges over 1 ns. In order to see if this is merely within the realm of what is conceivable, we carried out additional simulations, trying to characterize the conductance of larger pores. These were generated by performing simulations under a constant electric field, $\vec{E}$, perpendicular to the membrane patch, inducing a voltage of 2 V. For an MD run lasting about 2 ns, the diameter of the hydrophilic pore increased to $\sim$5 nm, enabling the conduction of $\sim$100 ions. This shows that it is indeed possible that the voltage drop events we observed in the experimental setup were due to the formation of a single pore, provided the latter has a diameter of a few nanometers.

Considering the experimental recordings (Fig. 5a) and given the shape of the voltage drops (and subsequent resealing), it seems more likely, however, that only a single pore is involved. The other alternative (hundreds of small pores within the experimental patch) would require that multiple pores would all open at the same time (on the millisecond time scale). There is even less rationale for the multiple pores to close all at the same time (millisecond time scale) while the transmembrane voltage keeps rising, i.e., as the electrical stress is becoming greater. On the contrary, if the events are due to a single pore, when the stress is relieved due to local ionic conduction in the region around the pore, the latter would close while the voltage keeps rising in the rest of the membrane. Such a scenario would lead eventually to breakdown of the planar lipid bilayer at U_{br}.

Electroporation is herein induced in the MD simulations by ionic salt concentration gradients between the two sides of the lipid bilayer patch, i.e., imposing a charge imbalance across the bilayer. One way of doing so is to consider in the MD simulation cell three salt baths separated by two bilayers and the use of 3D periodic boundary conditions at constant pressure. Accordingly, the overall lateral pressure on the system is zero. However, only one bilayer undergoes electroporation in such setups, and the influence of such asymmetry on the exact tension of the latter is not clear. Here, we performed a simulation considering a single bilayer and the air–water interface. In such a setup the simulation is carried out at constant volume, and therefore, a surface tension builds as the bilayer undergoes electroporation. We should note, however, that while this may be considered more appropriate for comparison to the planar lipid bilayer experimental setup, it is very difficult to estimate the lateral tension that builds up in the much larger bilayer patch.

In summary, we applied linear rising currents on planar POPC bilayers to observe well-defined voltage drops due to poration of the membrane. The use of theoretical tools, such as SPICE modeling and MD simulations, helped us to understand and characterize the phenomena occurring on a molecular scale and indicate that the observed voltage drops in bilayer patches are likely due to the opening and resealing of a single pore, a few tens of angstroms wide and of $\sim$100 nS conductance. Such a molecular understanding should enable better control and tuning of electroporation parameters to a wide range of biomedical and biotechnological applications.

Acknowledgements This work was in part supported by various grants from the Slovenian Research Agency and bilateral cooperation programs between Poland and Slovenia and between France and Slovenia (PROTEUS). The research was conducted in the scope of the EBAM European Associated Laboratory. Simulations were performed using HPC resources from GENCI-CINES (Grant 2010-075137). We thank A. Burmen for valuable discussion regarding SPICE modeling. M. T. acknowledges the support of the French Agence Nationale de la Recherche (Grant ANR-10_BLAN-916-03-INTCELL).

References

Benz R, Janko K (1976) Voltage-induced capacitance relaxation of lipid bilayer membranes: effects of membrane composition. Biochim Biophys Acta 455:721–738

Bockmann RA, de Groot BL, Kakorin S et al (2008) Kinetics, statistics, and energetics of lipid membrane electroporation studied by molecular dynamics simulations. Biophys J 95:1837–1850

Darden T, York D, Pedersen L (1993) Particle mesh Ewald—an n.log(n) method for Ewald sums in large systems. J Chem Phys 98:10089–10092

Delemotte L, Dehez F, Treptow W, Tarek M (2008) Modeling membranes under a transmembrane potential. J Phys Chem B 112:5547–5550

Essmann U, Perera L, Berkowitz M et al (1995) A smooth particle mesh Ewald method. J Chem Phys 103:8577–8593

Genco I, Gliozzi A, Relini A et al (1993) Electroporation in symmetric and asymmetric membranes. Biochim Biophys Acta 1149:10–18

Glaser R, Leikin S, Chernomordik L et al (1988) Reversible electrical breakdown of lipid bilayers—formation and evolution of pores. Biochim Biophys Acta 940:275–287

Golzio M, Teissie J, Rols M (2002) Direct visualization at the single-cell level of electrically mediated gene delivery. Proc Natl Acad Sci USA 99:1292–1297

Gurtovenko A, Vattulainen I (2005) Pore formation coupled to ion transport through lipid membranes as induced by transmembrane

ionic charge imbalance: atomistic molecular dynamics study. J Am Chem Soc 127:17570–17571
Gurtovenko A, Anwar J, Vattulainen I (2010) Defect-mediated trafficking across cell membranes: insights from in silico modeling. Chem Rev 110:6077–6103
Heller R, Gilbert R, Jaroszeski M (1999) Clinical applications of electrochemotherapy. Adv Drug Deliv Rev 35:119–129
Henin J, Shinoda W, Klein ML (2008) United-atom acyl chains for CHARMM phospholipids. J Phys Chem B 112:7008–7015
Jorgensen W, Chandrasekhar J, Madura J et al (1983) Comparison of simple potential functions for simulating liquid water. J Chem Phys 79:926–935
Kale L, Skeel R, Bhandarkar M et al (1999) NAMD2: greater scalability for parallel molecular dynamics. J Comput Phys 151: 283–312
Kalinowski S, Figaszewski Z (1995a) A 4-electrode system for measurement of bilayer lipid membrane capacitence. Meas Sci Technol 6:1043–1049
Kalinowski S, Figaszewski Z (1995b) A 4-electrode potentiostat-galvanostat for studies of bilayer lipid membranes. Meas Sci Technol 6:1050–1055
Kalinowski S, Ibron G, Bryl K, Figaszewski Z (1998) Chronopotentiometric studies of electroporation of bilayer lipid membranes. Biochim Biophys Acta 1369:204–212
Kandasamy SK, Larson RG (2006) Cation and anion transport through hydrophilic pores in lipid bilayers. J Chem Phys 125: 074901
Koronkiewicz S, Kalinowski S (2004) Influence of cholesterol on electroporation of bilayer lipid membranes: chronopotentiometric studies. Biochim Biophys Acta 1661:196–203
Koronkiewicz S, Kalinowski S, Bryl K (2002) Programmable chronopotentiometry as a tool for the study of electroporation and resealing of pores in bilayer lipid membranes. Biochim Biophys Acta 1561:222–229
Kotnik T, Bobanovic F, Miklavcic D (1997) Sensitivity of transmembrane voltage induced by applied electric fields—a theoretical analysis. Bioelectrochem Bioenerg 43:285–291
Kotnik T, Macek-Lebar A, Miklavcic D, Mir L (2000) Evaluation of cell membrane electropermeabilization by means of a nonpermeant cytotoxic agent. Biotechniques 28:921–926
Kotulska M, Koronkiewicz S, Kalinowski S (2004) Self-similar processes and flicker noise from a fluctuating nanopore in a lipid membrane. Phys Rev E 69:031920
Kotulska M, Kubica K, Koronkiewicz S, Kalinowski S (2007) Modeling the induction of lipid membrane electropermeabilization. Bioelectrochemistry 70:64–70
Kotulska M, Basalyga J, Derylo M, Sadowski P (2010) Metastable pores at the onset of constant-current electroporation. J Membr Biol 236:37–41
Kramar P, Miklavcic D, Lebar AM (2007) Determination of the lipid bilayer breakdown voltage by means of linear rising signal. Bioelectrochemistry 70:23–27
Kramar P, Miklavcic D, Lebar AM (2009) A system for the determination of planar lipid bilayer breakdown voltage and its applications. IEEE Trans Nanobiosci 8:132–138
Marty M, Sersa G, Garbay JR et al (2006) Electrochemotherapy—an easy, highly effective and safe treatment of cutaneous and subcutaneous metastases: results of ESOPE (European Standard Operating Procedures of Electrochemotherapy) study. EJC Suppl 4:3–13
Melikov K, Frolov V, Shcherbakov A et al (2001) Voltage-induced nonconductive pre-pores and metastable single pores in unmodified planar lipid bilayer. Biophys J 80:1829–1836
Mir LM, Banoun H, Paoletti C (1988) Introduction of definite amounts of nonpermeant molecules into living cells after electropermeabilization—direct access to the cytosol. Exp Cell Res 175:15–25
Mir L, Orlowski S, Belehradek J et al (1995) Biomedical applications of electric pulses with special emphasis on antitumor electrochemotherapy. Bioelectrochem Bioenerg 38:203–207
Montal M, Mueller P (1972) Formation of bimolecular membranes from lipid monolayers and a study of their electrical properties. Proc Natl Acad Sci USA 69:3561–3566
Neumann E, Rosenheck K (1972) Permeability changes induced by electric impulses in vesicular membranes. J Membr Biol 10: 279–290
Phillips J, Braun R, Wang W et al (2005) Scalable molecular dynamics with NAMD. J Comput Chem 26:1781–1802
Prausnitz MR, Bose VG, Langer R, Weaver JC (1993) Electroporation of mammalian skin—a mechanism to enhance transdermal drug-delivery. Proc Natl Acad Sci USA 90:10504–10508
Pucihar G, Mir L, Miklavcic D (2002) The effect of pulse repetition frequency on the uptake into electropermeabilized cells in vitro with possible applications in electrochemotherapy. Bioelectrochemistry 57:167–172
Rols M, Teissie J (1998) Electropermeabilization of mammalian cells to macromolecules: control by pulse duration. Biophys J 75:1415–1423
Sersa G, Cemazar M, Miklavcic D (1995) Antitumor effectiveness of electrochemotherapy with *cis*-diamminedichloroplatinum(II) in mice. Cancer Res 55:3450–3455
Tarek M (2005) Membrane electroporation: a molecular dynamics simulation. Biophys J 88:4045–4053
Tarek M, Delemotte L (2010) Electroporation of lipid membranes. In: Pakhomov A, Miklavčič D, Markov M (eds) Advanced electroporation techniques in biology and medicine. Taylor and Francis/CRC Press, Boca Raton, FL
Teissie J, Rols M (1993) An experimental evaluation of the critical potential difference inducing cell-membrane electropermeabilization. Biophys J 65:409–413
Teissie J, Eynard N, Gabriel B, Rols M (1999) Electropermeabilization of cell membranes. Adv Drug Deliv Rev 35:3–19
Teissie J, Escoffre JM, Rols MP, Golzio M (2008) Time dependence of electric field effects on cell membranes. A review for a critical selection of pulse duration for therapeutical applications. Radiol Oncol 42:196–206
Tieleman D (2004) The molecular basis of electroporation. Biophys J 86:371A–372A
Tieleman D, Leontiadou H, Mark A, Marrink S (2003) Simulation of pore formation in lipid bilayers by mechanical stress and electric fields. J Am Chem Soc 125:6382–6383
Tien HT (1974) Bilayer lipid membranes. Marcel Dekker, New York
Tuma T, Buermen Á (2009) Circuit simulation with SPICE OPUS: theory and practice. Birkhäuser, Boston
Villemejane J, Mir LM (2009) Physical methods of nucleic acid transfer: general concepts and applications. Br J Pharmacol 157: 207–219
Ziegler MJ, Vernier PT (2008) Interface water dynamics and porating electric fields for phospholipid bilayers. J Phys Chem B 112:17003
Zimmermann U, Pilwat G, Beckers F, Riemann F (1976) Effects of external electrical fields on cell-membranes. Bioelectrochem Bioenerg 3:58–83